

1 **Wetter environment and increased grazing reduced the area burned in northern Eurasia: 2002 –**
2 **2016**

3 Wei Min Hao¹, Matthew C. Reeves², L. Scott Baggett³, Yves Balkanski⁴, Philippe Ciais⁴, Bryce
4 L. Nordgren¹, Alexander Petkov¹, Rachel E. Corley¹, Florent Mouillot⁵, Shawn P. Urbanski¹,
5 Chao Yue⁶

6
7 ¹United States Forest Service, Rocky Mountain Research Station, Fire Sciences Laboratory, 5775
8 Highway 10 West, Missoula, MT 59808 USA.

9 ²United States Forest Service, Rocky Mountain Research Station, Forestry Sciences Laboratory,
10 800 E. Beckwith, Missoula, MT 59801, USA.

11 ³United States Forest Service, Rocky Mountain Research Station, 240 West Prospect, Fort
12 Collins, CO 80526, USA.

13 ⁴Laboratoire des Sciences du Climat et de l'Environnement, LSCE CEA CNRS UVSQ, 91191
14 Gif Sur Yvette, France.

15 ⁵UMR CEFE 5175, Centre National de la Recherche Scientifique (CNRS), Université de
16 Montpellier, Université Paul-Valéry Montpellier, Ecole Pratique des Hautes Etudes (EPHE),
17 Institut de Recherche pour le Développement, 34293 Montpellier CEDEX 5, France.

18 ⁶Institute of Soil and Water Conservation, Northwest A&F University, Yangling, Shaanxi
19 712100, P.R. China.

20

21 **Correspondence:** Wei Min Hao (weimin.hao@usda.gov)

22

23 **Abstract.** Northern Eurasia is currently highly sensitive to climate change. Fires in this region
24 can have significant impacts on regional air quality, radiative forcing and black carbon
25 deposition in the Arctic to accelerate ice melting. Using a MODIS-derived burned area data set,
26 we report that the total annual area burned in this region declined by 53 % during the 15-year
27 period of 2002–2016. Grassland fires dominated this trend, accounting for 93 % of the decline of
28 the total area burned. Grassland fires in Kazakhstan contributed 47 % of the total area burned
29 and 84% of the decline. Wetter climate and increased grazing are the principle driving forces for
30 the decline. Our findings: 1) highlight the importance of the complex interactions of climate-
31 vegetation-land use in affecting fire activity, and 2) reveal how the resulting impacts on fire
32 activity in a relatively small region such as Kazakhstan can dominate the trends of burned areas
33 across a much larger landscape of northern Eurasia.

34 **1 Introduction**

35 Fire activity worldwide is very sensitive to climate change and human actions, especially over
36 high latitude ecosystems (Goetz et al., 2007). Identifying and unraveling confounding drivers of
37 fire is critical for understanding the recent and future impacts of fire activity. In northern Eurasia
38 fire activity impacts of chief concern include carbon cycling, boreal ecosystem dynamics, fire
39 emissions (Hao et al., 2016a), accelerated ice melting in the Arctic (Hao et al., 2016a;
40 Evangeliou et al., 2016), early thawing of permafrost, and the hydrological cycle in high-
41 latitudes (IPCC, 2014). In addition, it affects air quality in Europe, Asia and North America. An
42 improved understanding of the region's fire dynamics can also be applied to develop climate

43 change mitigation policy and be incorporated into the fire modules of Earth System Models to
44 improve their predictions (Hantson et al., 2016).

45 Global mean surface temperature rose by approximately 0.72° C from the year 1951 to 2012
46 according to the 5th Intergovernmental Panel on Climate Change Report (IPCC) (IPCC, 2013),
47 but remained relatively constant (“warming slowdown”) from 1998 to 2013 (Fyfe et al., 2013;
48 Cowtan and Way, 2014; Trenberth et al., 2014; Fyfe et al., 2016). Nevertheless, extreme high
49 temperature events continued to occur even during the warming slowdown (Seneviratne et al.,
50 2014; Trenberth et al., 2015). Since 2013, the global temperatures have risen rapidly (NASA
51 Global Climate Change, 2019) and there were hemispheric temperature anomalies from 1850 to
52 2015 (Jones et al. 2016). In the Northern Hemisphere, temperatures have increased more
53 profoundly than in the Southern Hemisphere since the 1980’s, as they are greatly affected by the
54 sources of greenhouse gases and any other factors. High latitudes are projected to have the
55 largest temperature increase globally by 2100 (IPCC, 2013). At the same time, however, climatic
56 components of the fire weather index (FWI), an index of fire intensity potential, have
57 experienced regional divergence at these latitudes with a positive FWI trend in Eastern Asia and
58 a negative trend in Kazakhstan (Jolly et al. 2015), suggesting divergent regional climate impacts.
59 In northern Eurasia, current accelerated high temperatures in the summer were also observed in
60 Eastern European Plain and Central Siberia (Sato and Nakamura, 2019).

61 Over the past 20 years, the decline of total area burned in Eurasia has been observed (Giglio et
62 al., 2013; Hao et al., 2016a and Andela et al., 2017). We will investigate trends in the spatial and
63 temporal distribution of area burned from 2002 to 2016 across different land cover types and
64 geographic regions of northern Eurasia, a region highly sensitive to climate change. The
65 geographic subregion with the largest declining trend is examined and the influence of the
66 confounding factors of climate and human activity on burned area is explored.

67 Our study seeks to evaluate the decline in burned area as a function of variable fuel conditions
68 (Krawchuk and Moritz 2011), land use and relative moisture conditions (Pausas and Ribeiro
69 2013). Beside these climate variables, abrupt changes have been observed globally to
70 significantly impact long-term or recent fire history (Pausas and Keeley 2014), among other
71 mechanisms, such as herbivory from native and domestic ungulates and humans (e.g. fire
72 prevention). Considerable research has been done to understand climate-fire-grazing interactions
73 in grassland ecosystems. In grasslands, reductions in fuel availability due to decreasing net
74 primary production, grazing or other management activities can be the key variables limiting fire
75 spread (Moritz et al., 2005). For instance, in the western United States, the research has
76 significant implications on forest and rangeland management (e.g. Bachelet et al., 2000; Gedalof
77 et al., 2005; Riley et al., 2013; Abatzoglou and Kolden, 2013). Similar issues were investigated
78 on African savanna for maintaining sustainable grassland (e.g. Archibald et al., 2009; Koerner
79 and Collins, 2014). In this study we closely examine the interactions of climate, fire, grazing and
80 fuel availability in Kazakhstan, the country of northern Eurasia with the largest decline in burned
81 area during 2002–2016.

82 **2 Methodology**

83 **2.1 Study area**

[Type here]

84 First, we study the area of northern Eurasia, a region from 35° N to the Arctic and from the
85 Pacific Ocean to the Atlantic Ocean. The region comprises 21 % of the Earth's land area and
86 encompasses diverse ecosystems from the steppes of central Asia to the Arctic. Forest is the
87 major ecosystem in this region covering 27 % of the area, followed by grasslands which cover 16
88 % (Friedl et al., 2010).

89 Second, to understand the forces driving the decline of burned area, we focus on the effects of
90 drought and grazing in Kazakhstan. From 2002 to 2016, Kazakhstan had the highest rate of
91 decline in burned area in northern Eurasia (see Figs. 1 and 2). In Kazakhstan, grassland is the
92 dominant ecosystem and grazing is the major agricultural activity (Food and Agriculture
93 Organization FAO Live Animals Database, 2016).

94 **2.2 Mapping burned areas**

95 **Burned area in northern Eurasia**

96 Since 2000, global burned area has been mapped by remote sensing (e.g. Mouillot et al. 2014)
97 with different sensors and detection algorithms (Chuvieco et al., 2019), leading to multiple
98 datasets with a significant uncertainty in the magnitude of spatial distribution, interannual
99 variability and trends in burned area (Hantson et al., 2016). We used daily NASA MODIS
100 (Moderate Resolution Imaging Spectroradiometer) dataset at a 500 m × 500m resolution. Our
101 MODIS-derived burned area algorithm was validated in eastern Siberia with the Landsat derived
102 burned area (30 m × 30 m) (Hao et al., 2012). The ratio of these two satellite derived burned
103 areas was 1.0 with a standard deviation of 0.5 % over 18,754 grid cells. Among other sources of
104 variability, surface and crown fires generate significantly different spectral signals, so that the
105 detection algorithm depends on vegetation type classification (Chuvieco et al., 2019).

106 The burned area data were analyzed at multiple spatial and temporal scales using frequentist
107 statistical methods (see section 2.4) to identify regional trends. Assessing burned area changes in
108 northern Eurasia over this time period benefits from the lack of fire suppression in this region
109 (Goldammer et al., 2013), so the impact of climate and land use on fire activity can be better
110 understood. Our methodology for mapping daily burned area is very similar to that used by Hao
111 et al. (2016a, 2016b) which was specifically developed for this region. For the study of Hao et al.
112 (2016a, 2016b), the MCD12Q1 land cover map of 2015 was used for 2002–2016. For this
113 present study, a timely-consistent and up-to-date land cover product was used for 2002–2013 and
114 the 2013 land cover map was used for 2014–2016 because current versions were not available
115 for present and previous studies

116 **2.3 Data sources of drought, livestock, annual biomass production, and land cover**

117 The following data sources for estimating the factors affecting the burned area in Kazakhstan are
118 described below: drought, livestock, annual biomass production, and land cover. All data were
119 evaluated at the county level for 174 counties during the period of 2002–2016 (Fig. 1). We
120 focused on Kazakhstan as it was the region with the largest decline of burned area in northern
121 Eurasia (see section 3.1).

122 **Drought**

123 The Palmer Drought Severity Index (PDSI) from the TerraClimate site
124 (<http://www.climatologylab.org>) was used to estimate drought throughout Kazakhstan
125 (Abatzoglou et al., 2018). The PDSI was developed by Palmer (1965) and is widely used to
126 estimate a rough soil water budget based on monthly precipitation, potential evapotranspiration
127 with varying soil property of available water content to account for pedological variations and
128 species roots access to water. We used monthly PDSI data from March to July, defined as the
129 fire season (Roy et al., 2008), to compute a cumulative drought effect index. The gridded PDSI
130 data were available at a spatial resolution of ~ 4 km and were aggregated to the county within the
131 study area (Fig. 1). PDSI varies from + 4 for wet conditions to - 4 for dry conditions.

132 **Livestock**

133 The annual population of livestock in each of the 14 provinces, each consisting of multiple
134 counties, of Kazakhstan from 2002 to 2016 were compiled by the official agriculture statistics of
135 the Ministry of National Economy of the Republic of Kazakhstan Committee on Statistics
136 (MANE, 2019). These data included yearly numbers of large horned livestock and sheep and
137 goats at the province level which is coarser than the counties. Livestock populations are only
138 available at the province level and the population was distributed proportionally to the size of the
139 county area so that all potential drivers of fire activity could be evaluated on a common spatial
140 scale. The livestock density for each county is therefore defined as the ratio of the number of
141 animals to the area of the county.

142 **Annual biomass production**

143 We estimated the annual biomass production within the grassland domain of the study area (Fig.
144 2) using the production subroutine of the Rangeland Vegetation Simulator model (RVS) (Reeves
145 2016) which applied the methods of Reeves et al. (in press). The RVS, which was originally
146 developed for simulating rangeland vegetation dynamics in the continental United States, models
147 annual production based on MODIS normalized difference vegetation index (NDVI) at a 250 m
148 spatial resolution (MOD13Q1). The MOD13Q1 NDVI data are composited on a bi-weekly basis
149 and are available at a spatial resolution of 250 m. The QA/QC flags were used to isolate only the
150 best quality NDVI pixels. At each pixel, the highest quality maximum value composite on an
151 annual basis was retained for further analysis. The relationships between the estimates of annual
152 net primary production (ANPP) and maximum NDVI were divided into two groups to enable
153 different models to be fit to the lower and upper end of production given as

$$154 \quad y = 240.31 * e^{3.6684 x} \quad (1)$$

155 where y is the estimated ANPP in kg ha^{-1} of dry weight and x is the NDVI for the upper range (x
156 ≥ 0.46) and

$$157 \quad y = 971.1 * \ln x + 1976 \quad (2)$$

158 where y is the estimated ANPP in kg ha^{-1} and x is the NDVI for the lower range ($x < 0.46$). The
159 partition into 2 groups was done, in part, because of the asymptotic nature or “saturation” feature
160 (Santin-Janin et al., 2009) of NDVI with respect to ANPP.

161 **Land cover**

162 The MODIS land cover product (MCD12Q1) Version 6 was used to assess factors affecting the
163 burned area in Kazakhstan. The product is available at a 500 m spatial resolution and describes
164 the distribution of broad vegetation types. We screened these data to subset only those vegetation
165 types considered to represent grassland vegetation (Class 10 in the MCD12Q1 dataset) from
166 2000 to 2016. In each year of the assessment, the number of grassland pixels was summed to
167 enable estimates of grassland area throughout the study area.

168 **2.4 Statistical analysis**

169 For each pixel of $0.5^\circ \times 0.5^\circ$, the annual trend (Fig. 2) was estimated as the robust linear slope
170 computed from burned area on year using M-estimation as described in Huber (1981). Our
171 objective was to present consistent grid cell trends in the presence of within-cell variation. We
172 chose to use M-estimation to mitigate the effect of large within-cell variation due to a relatively
173 small within-cell sample such that the map presents a consistent surface. If computed using
174 ordinary least squares (OLS) estimates, such large within-cell variation could result in some cells
175 with inconsistent or "outlier" trends compared to their neighbors. The trends were estimated
176 using the R platform (R Core Team, 2019) with R function *rlm* in package MASS (Venables and
177 Ripley, 2002). Pairwise robust rank correlations (Fig. 5, 6) were computed as described in
178 Kendall (1938) using the R function *cor*.

179 To validate our estimates on burned areas, we compare of our annual northern Eurasia burned
180 areas (FEI-NE) with the latest version of the MODIS burned area product (MCD64A1, collection
181 6) (Giglio et al., 2018) from 2002 to 2016 (Fig. 3). The burned areas reported by FEI-NE and
182 MODIS MCD64 were each modeled separately by year. The models each include a first-order
183 autoregressive term on the residuals to account for the presence of temporal autocorrelation. The
184 response was assumed to be gamma distributed (Bickel and Doksum, 2015). A generalized linear
185 mixed model (GLMM) approach was used and estimated using the R function *glmmTMB* in
186 platform (R Core Team, 2019) with R package *glmmTMB* (Brooks et al., 2017).

187 The potential driving forces of burned area at the county level for 174 counties over a period of
188 15 years from 2002 to 2016 were modeled using the GLMM approach to interpret the effects on
189 the extent of the area burned. The proportion of burned area per county was modeled on the
190 effects of year, PDSI during the fire season (May-July), proportion of grass area, ANPP and
191 livestock density along with two-way interactions. The model included a random effect that
192 accounts for spatial correlation within each region along with a first-order autoregressive term on
193 the residuals within each county that accounts for temporal autocorrelation. The response was
194 assumed to be beta distributed (Bickel and Doksum, 2015). The model was estimated using the R
195 function *glmmTMB* in platform (R Core Team, 2019) with R package *glmmTMB* (Brooks et al.,
196 2017).

197 **3 Results**

198 3.1 Spatial and temporal distribution of burned areas in northern Eurasia

199 The declining trends in the spatial distribution of the area burned from 2002 to 2016 in northern
 200 Eurasia at a $0.5^\circ \times 0.5^\circ$ resolution are shown in Fig. 2. The majority of the area burned was
 201 grassland of Kazakhstan in central Asia. However, substantial areas were also burned in the
 202 Russian Far East along the Chinese border because of illegal logging (Vandergert and Newell,
 203 2003) and the subsequent fires to burn the remaining forest residues. The annual areas burned
 204 according to ecosystem and geographic region are summarized in Table 1. The interannual
 205 burned area in northern Eurasia varied about four times within a range from $1.2 \times 10^5 \text{ km}^2$ in
 206 2013 to $5.0 \times 10^5 \text{ km}^2$ in 2003 with an average of $(2.7 \pm 1.0) \times 10^5 \text{ km}^2$ ($n = 15$). Grassland
 207 accounted for 71 % of the total area burned, despite comprising only 16 % of the land cover
 208 (Friedl et al., 2010). Almost all the grassland fires occurred in Kazakhstan in central and western
 209 Asia (Table 1). In contrast, forest is the major ecosystem that covers 27 % of northern Eurasia
 210 (Friedl et al., 2010), but contributes only 18 % of the total area burned. About ninety percent of
 211 the forest area burned occurred in Russia.

212 3.2 Trends of burned areas in northern Eurasia

213 Comparisons of our annual northern Eurasia burned areas (FEI-NE) with the latest version of the
 214 MODIS burned area product (MCD64A1, collection 6) (Giglio et al., 2018) from 2002 to 2016
 215 are shown in Fig. 3. The burned areas in these two datasets agree better in recent years after
 216 2010. Both FEI-NE and MCD64A1 demonstrated declining trends and similar interannual
 217 variability. The FEI-NE dataset was used to analyze the driving forces for the decline of burned
 218 area in Kazakhstan (see sections 3.3–3.4).

219 Grasslands of Kazakhstan dominate changes in burned area with significant declines mostly in
 220 central and northern Kazakhstan, adjacent to the Russian border. The temporal trend of annual
 221 burned areas over all vegetation types and in grasslands in northern Eurasia and in Kazakhstan
 222 from 2002 to 2016 are shown in Fig. 4. The burned area trends shown in Fig. 4 were modeled
 223 like that reported in Fig. 3 with the same response distribution. The trends of wave-like burned
 224 areas are typical for burned area trends in the world (e.g. Andela et al., 2017). The annual total
 225 area burned over northern Eurasia during this period decreased by 53% from $3.3 \times 10^5 \text{ km}^2$ in
 226 2002 to $1.6 \times 10^5 \text{ km}^2$ in 2016 (Table 1), or at a rate of $1.2 \times 10^4 \text{ km}^2$ (or 3.5 %) yr^{-1} . The
 227 grassland area burned during the 15 years declined by 74 % from $2.8 \times 10^5 \text{ km}^2$ in 2002 to $7.3 \times$
 228 10^4 km^2 in 2016, or at a rate of $1.3 \times 10^4 \text{ km}^2$ (or 4.9 %) yr^{-1} . Grassland fires in Kazakhstan
 229 accounted for 47 % of the total areas burned but contributed 84 % of the declining trend. The
 230 annual forest burned area varied by a factor of 5 from 21,243 km^2 in 2010 to 111,019 km^2 in
 231 2003, but there is no trend over the 15 years (Table 1).

232 233 3.3 Regional trends in driving forces over time in Kazakhstan

234 One of our objectives was to evaluate trends in the primary drivers responsible for reducing area
 235 burned, especially in grasslands at the county level. Pairwise correlation results are shown in Fig.
 236 5. Each panel of Fig. 5 illustrates the coefficient of correlation between a key variable and year
 237 (2002–2016) for the 174 counties of Kazakhstan. The major factors affecting the trend of area
 238 burned in Kazakhstan are wetter climate (represented as PDSI), the proportion of grassland

239 cover, ANPP and livestock density (Table 2). Both grassland partition and ANPP enable
240 spreading fires.

241 The declining trends in the fraction of the area burned annually are shown in Fig. 5a. The trend
242 of PDSI from March to July during the 15-year period is illustrated in Fig. 5b. A higher PDSI
243 value indicates a wetter environment. Increasing wetness, i.e. higher PDSI, during the fire season
244 reduces the probability of fire ignition and fire spread. The declining trend of the burned area
245 (Fig. 5a) is then consistent of the increasing trend of PDSI (wet conditions) especially in central
246 and southern Kazakhstan (e.g. East Kazakhstan, Qaraghandy, Zhambyl, Almaty) (Fig. 5b).

247 Through time the proportion of grassland cover has been asymmetric with some counties having
248 exhibited strong decreases such as in the north central region of Kazakhstan, while others have
249 seen increases such as in the north western region (Fig. 5c). This north central region has also
250 exhibited decreases in burned area (Fig. 5a). Similarly, some regions have shown increasing
251 trends of grassland cover through time without commensurate increases in the proportion of
252 burned area (Figs. 5a and 5c).

253 The impacts of year, PDSI, land cover, ANPP and livestock density on the extent of the area
254 burned and the correlations of burned area with these driving forces are illustrated in Fig. 6. Area
255 burned and PDSI were negatively correlated in most of the counties in Kazakhstan (Fig. 6b).
256 Therefore, as Kazakhstan becomes wetter during the fire season, the area burned declined over
257 the 2002–2016 period. At the same time, grassland cover decreased across most of Kazakhstan,
258 with a notable exception being the north central region and south western region (Fig. 6c). ANPP
259 decreased with time over most of Kazakhstan, the exception being central and south western
260 counties (Fig. 6d).

261 Finally, we investigated livestock density as a potential non-climatic driver affecting fuel
262 amount. The population density of livestock increased with time in all counties and was greatest
263 in the central, northern and southern counties of Qostanay, Pavlodar and Qaraghandy (Fig. 5e).
264 The coupling of livestock density with PDSI affected the extent of the area burned (Fig. S1.4)
265 with $p = 0.042$ (Table 2). The area burned was negatively correlated with the population of
266 livestock throughout nearly all of Kazakhstan (Fig. 6e). This observation suggests the increasing
267 population of grazing livestock may have reduced fuelbed continuity contributing to the decrease
268 of the area burned in Kazakhstan. Since 2000, the numbers of sheep, goats and cattle have
269 increased by 60% in Kazakhstan based on MANE statistics (2019) (Figs. S2 and S3). Thus,
270 increased livestock grazing could decrease the amount of herbaceous fuel across the landscape
271 and offset increases in fuel quantity due to expanded grassland cover. The net result would be
272 reductions in fire spread and the area burned.

273 **3.4 Interactions of driving forces**

274 The driving forces (e.g. year, PDSI, proportion of grassland cover, ANPP, livestock density) for
275 the decline of the burned areas in Kazakhstan from 2002 to 2016 are inter-related. It is therefore
276 critical to evaluate their interactions. For instance, Figures S1.1–S1.4 illustrate the proportion of
277 burned area affected by the interactions of the driving forces at 174 counties over 15 years in
278 Table 2.

279 **Proportion of grassland cover and year** – Both year and the proportion of grassland area had
280 significant effects on burned area when interacted (Table 2, $p < 0.001$). When the proportion of
281 grassland cover in a county is very low (e.g. 0.48 %), only about 0.6 % of the area was burned
282 annually during the period of the year 2002 to 2016 (Fig. S1.1, upper left panel). On the contrary,
283 while the grassland cover is 25 % or greater, the area burned declined steadily from 1.5 % in the
284 year 2000 to 0.6 % in 2016 (Fig. S1.2 lower right panel). This observation is consistent with
285 grassland enhancing the spread of fires in the absence of opposing factors.

286 **PDSI and proportion of grassland area** – Both PDSI and the proportion of grassland area had
287 significant effects on burned area when interacted (Table 2, $p = 0.028$). As in Fig. S1.2, for PDSI
288 in a range of -4.5 to ~ 2, the percentage of the area burned remained about 0.6 % for grassland
289 area of 0.5 % (upper left panel). On the other hand, when grassland cover of 60 %, the fraction of
290 area burned declined from 2.2 % to 0.8 % (lower right panel). This analysis is consistent with
291 grassland enhancing the spread of fires, as in the previous section of proportion of grassland
292 cover through time, and illustrates that increasing wetness significantly decreases burned area
293 mostly when grassland cover is high.

294 **Livestock density and year** – We investigated livestock density as a potential non-climatic
295 driver affecting fuel amount and area burned. The effects of grazing on the area burned during
296 2002 – 2016 are shown in Table 2, $p = 0.089$. The declining trend of the area burned with time
297 for different livestock density are illustrated in Fig. S1.3. Higher livestock density results in less
298 available biomass to burn and the less area burned (lower right panel). It provides additional
299 evidence that grazing could reduce the area burned in Kazakhstan.

300 **PDSI and livestock density** – The interaction between PDSI and livestock was significant to
301 affect the area burned ($p = 0.042$). Figure S1.4 shows the decline in the proportion of burned area
302 with PDSI at different livestock densities. As PDSI increases (wetter landscape), less area is
303 burned. However, the declining trends differ with livestock density. This relationship is quite
304 different for the livestock density of 0.002 heads km^{-2} (Fig. S1.4 upper left panel) and 0.05 heads
305 km^{-2} (Fig. S1.4 lower right panel). For instance, for low PDSI (-4, dry), 1.5 % of the area was
306 burned for all livestock densities. In contrast, at high PDSI (+2, wet), the percentage of burned
307 area decreases with increasing livestock density. Thus, during dry years the area burned is
308 unaffected by grazing intensity, but during wet years with high biomass (based on our RVS
309 analysis of Reeves, 2016), high grazing intensity tends to decrease burned area.

310 **4 Discussion**

311 **Burned area**

312 The spatial and temporal extent of the area burned were examined in different ecosystems in
313 northern Eurasia from 2002 to 2016, during which the average area burned was $(2.7 \pm 1.0) \times 10^5$
314 $\text{km}^2 \text{yr}^{-1}$. The burned area in grasslands declined 74 % from ~ 282,000 km^2 in 2002 to ~ 73,000
315 km^2 in 2016 at a rate of $1.3 \times 10^4 \text{km}^2 \text{yr}^{-1}$. The area burned in forest showed no trend over time.
316 Our burned area is higher than the MODIS MCD64 collection 6, in which the average annual
317 burned area was $9.7 \times 10^4 \text{km}^2$ in boreal Asia during the same period (Giglio et al., 2018).
318 Boreal Asia of MCD64 has a similar geographic region as our northern Eurasia. Nevertheless,
319 the interannual variability and the trends of burned area for the two datasets are consistent (Fig.
320 3).

321 Our results on burned area trends are consistent with other published results (Giglio et al., 2013;
322 Hao et al., 2016a; Andela et al., 2017) that concluded the area burned in northern Eurasia
323 declined, contrary to the projections of increased fire frequency driven by climate change
324 (Groisman et al., 2007; Kharuk et al., 2008). Uncertainty in global burned area remains a critical
325 challenge with trends and interannual variability reported by sensors and processing algorithms
326 exhibiting large differences (Hantson et al., 2016; Chuvieco et al., 2019).

327 **Grassland fires and grazing**

328 Grassland fires in Kazakhstan accounted for 47 % of the total area burned but comprised 84 % of
329 the decline of the total area burned in northern Eurasia during the 15 years of 2002–2016. The
330 grassland fires are human caused to produce fresh grass for grazing (Lebed et al., 2012) with a
331 cycle of about every two years. A similar temporal pattern characterizes grassland fire
332 occurrence in the African savanna (Hao and Liu, 1994; Andela and van der Werf, 2014).

333 Central Asia experienced tremendous socioeconomic change, with the collapse of the Soviet
334 Union in the 1990's leading to a full restructure of the agricultural system, followed by a rapid
335 collapse of cattle industry that has progressively recovered in the last 20 years (Figs. S2 and S3,
336 Food and Agriculture Organization, 2016). This change has potentially altered fuel availability to
337 burn as observed in other ecosystems (Robinson and Milner-Gulland, 2003; Holdo et al., 2009;
338 Vigan et al., 2017). The coincident decline in burned area with increasing livestock population
339 suggests changing agricultural practices may have exerted an influence on fire activity in
340 Kazakhstan and northern Eurasia. In addition, the relationship between livestock population and
341 the burned area was observed in arid grassland in a small region of southern Russia from 1986 to
342 2006 (Dubinin et al., 2011). During this time period, the livestock population was negatively
343 correlated with the area burned.

344 The fire activity data for Kazakhstan and Mongolia can be estimated from 1985 to 2017 as
345 shown in Fig. 7 based on the recently released AHVRR long term fire history (Otón et al., 2019).
346 This new information extends the analysis before our observed decrease during the 2002–2016
347 period and shows that fire activity increased in Kazakhstan just during the economic collapse
348 and the associated reduction of livestock in the year 2000. This opposite trend supports our
349 interpretation on the relationship between grazing and burned area, particularly when this
350 variation in burned area is not clearly observed in neighboring Mongolia where grazing collapse
351 did not occur.

352 In the steppe of neighboring Mongolia, overgrazing also affected fire activity from 1988–2008
353 (Liu et al., 2013) in a manner similar to Kazakhstan. However, extreme winter freezing and
354 inadequate preparation affected the increasing livestock trend driven by the poorly prepared
355 feeding of hay and foliage. It led to livestock reductions during the colder season than the
356 average period during the years of 2000 to 2014 (Nandintsetseg et al., 2018), highlighting the
357 potential impact of climate on livestock population beside human decisions and practices (Xu et
358 al., 2019).

359 We investigated grazing and land use as the main drivers of changes in fuel availability in
360 grasslands to abruptly impact fire regime as observed for Africa (Holdo et al., 2009; Andela et

361 al., 2017) or globally over long periods (Marlon et al., 2008). Political changes can be associated
362 to additional human processes affecting fire activity or fire spread. Among others, decreasing
363 population density (-10% observed in Kazakhstan after 1991) could decrease fire activity or
364 suppression effort and firefighting capacities as mentioned for the post-Soviet period (Mouillot
365 and Field, 2005), as well as local conflicts potentially exacerbating fire ignitions as observed in
366 Africa (Bromley 2010). These effects might contribute less significantly than the direct effect of
367 grazing and land use on fuel loading and the subsequent fire activity in the region. Gathering
368 social information remains a challenge to better apprehend human impact on fire activity.

369 **Modelling fire and grazing interactions**

370 Accounting for confounding factors related to burned area and the subsequent effects on
371 ecosystems, biosphere/atmosphere interactions and climate have been a challenge in developing
372 fire modules in global vegetation models (Hantson et al., 2016). Climate (drought, temperature
373 and humidity), land cover and fuel amount are the main drivers related to fire activity in
374 Dynamic Global Vegetation Models (DGVMs) coupled with human-related information as
375 population density and countries' wealth (Gross Domestic Product). Our understanding of land
376 use dynamics (Prestele et al., 2017), especially forest management, fire prevention and grazing
377 practices, is still developing (Rolinski et al., 2018) and better data assemblage and modeling
378 processes are needed (Pongratz et al., 2018). In our study, we showed the strong impact of
379 political events (here the collapse of the political regime) on grazing intensity and the subsequent
380 effect on fire activity. These stochastic events are hard to forecast and simulate so that DGVM
381 cannot fully capture long term trends in burned area (Kloster et al., 2010; Yue et al., 2014) when
382 compared to observed burned area reconstructions (Mouillot and Field 2005).

383 The Soviet economic collapse provides fruitful information on potential amplitude and impact of
384 grazing changes on ecosystem functioning. The 1998 Russian Financial Crisis led to dramatic
385 decrease of consumption of livestock in neighboring countries such as in Kazakhstan. Both sheep
386 and goats (Fig. S2) and cattle (Fig. S3) declined substantially from 1992 to 1998. As the
387 economy improved after late 1990s, the consumption of livestock has grown steadily. Integrating
388 grazing in DGVM has recently emerged for global models (Chang et al., 2013; Pachzelt et al.,
389 2015; Dangal et al. 2017) and for local studies (Bachelet et al., 2000; Caracciolo et al., 2017;
390 Vigan et al., 2017). Grazing processes as implemented in DGVMs can capture climate impact on
391 livestock populations which could be affected by climate extremes (Nandintsetseg et al., 2018)
392 and lack of forage or water (Tachiiri and Shinoda 2012; Vrieling et al., 2016). They still lack
393 abrupt and stochastic changes in projections of socio-economic processes, or infectious disease
394 potentially affecting livestock density as shown in Africa by Holdo et al. (2009) after rinderpest
395 curation.

396
397 Paleo-fire reconstructions already captured grazing as a keystone process through dung fungi
398 spore residuals in sediments (Cordova et al. 2019). Current modelling developments cover
399 disease projections (Perry et al. 2013), and increasingly, modelling efforts are devoted to the
400 more complex human aspect, including human consumption behavior, inequality and subsequent
401 potential issues (Motesharrei et al. 2016) or social conflicts (Neumann et al. 2011). Our study
402 demonstrates that grazing can be highly variable as a fast response or abrupt change in

403 agricultural policies or political regime. These abrupt changes can have a significant impact on
404 fire activity. Better integration of human process on grazing activities in DGVMs, even as
405 stochastic events, would capture this important process to account for probable political
406 collapse/agricultural policies, societal decisions or widespread animal diseases. These
407 improbable factors could affect future global carbon budget.

408 **5 Conclusions**

409 The spatial and temporal extent of the area burned was examined in different ecosystems in
410 northern Eurasia from 2002 to 2016. We conclude:

411 The burned area in grasslands declined 74 % from ~ 282,000 km² in 2002 to ~ 73,000 km² in
412 2016 or at a rate of 1.3×10^4 km² yr⁻¹. The area burned in forest did not show a trend. Grassland
413 fires in Kazakhstan accounted for 47 % of the total area burned but comprised 84 % of the
414 decline of the total area burned in northern Eurasia during the 15 years. Wetter climate and the
415 increase of grazing livestock in Kazakhstan are the major factors contributing to the decline of
416 the area burned in northern Eurasia. The population of livestock increased in most of Kazakhstan
417 from 2002 to 2016, decreasing the burned area by fuel removal from grazing. The major factors
418 affecting the availability of the fuels for the decline of burned area are climate, proportion of the
419 grassland cover, aboveground net primary production and livestock density. These factors
420 interact to reduce the area burned in Kazakhstan, especially in grassland.

421
422 *Data availability.* All data and materials are available in the manuscript or the supplementary
423 materials. The original geospatial dataset of the burned area is large and will be available upon
424 reasonable request. However, a derived dataset has been used to estimate black carbon emissions
425 from fires in the same region. It has been archived at the Forest Service Data Archive web site
426 (Hao et al., 2016b). <https://www.fs.usda.gov/rds/archive/Product/RDS-2016-0036/>

427
428 *Supplement.* The supplement for this article is available online at: xxx.

429
430 *Author contributions.* W.M.H. led the project and led writing the manuscript. M.C.R. simulated
431 aboveground biomass ANPP and advised statistical analysis. L.S.B. was responsible for
432 statistical analysis. Y.B., P.C. and F.M. suggested the use of PDSI and livestock population to
433 explain the declining burned areas. B.N. analyzed the data and contributed certain figures. A.P.
434 mapped burned areas., R.E.C. conducted GIS analysis. S.P.U. advised the execution of the
435 project. C.Y. advised on the trend of the burned areas. All authors contributed the writing of the
436 manuscript

437
438 *Competing interests.* The authors do not have competing interests.

439
440 *Acknowledgements.* W.M.H. received funding from the US Department of State, US Forest
441 Service Research and Development, and NASA Terrestrial Ecology Program. Y.B. and P.C.
442 have received funding from the European Union's Horizon 2020 research and innovation
443 program under grant agreement No 641816 (CRESCENDO). F.M. received funding from ESA
444 FIRECCI program.

445

446 **References**

447

448 Abatzoglou, J. T. and Kolden, C. A.: Relationships between climate and macroscale area burned
449 in the western United States, *International Journal of Wildland Fire*, 22, 1003–1020,
450 <http://dx.doi.org/10.1071/WF13019>, 2013.

451 Abatzoglou, J. T., Dobrowski, S. Z., Parks, S. A., and Hegewisch, K. C.: Terraclimate, a high-
452 resolution global dataset of monthly climate and climatic water balance from 1958-2015, *Sci*
453 *Data*, 5, 170191, <https://doi.org/10.1038/sdata.2017.191>, 2018.

454 Andela, N. and van der Werf, G. R.: Recent trends in African fires driven by cropland expansion
455 and El Niño to La Niña transition, *Nature Clim Change*, 4, 791-795,
456 <https://doi.org/10.1038/nclimate2313>, 2014.

457 Andela, N., Morton, D. C., Giglio, L., Chen, Y., van der Werf, G. R., Kasibhatla, P. S., DeFries,
458 R. S., Collatz, G. J., Hantson, S., Kloster, S., Bachelet, D., Forrest, M., Lasslop, G., Li, F.,
459 Mangeon, S., Melton, J. R., Yue, C., and Randerson, J. T.: A human-driven decline in global
460 burned area, *Science*, 356, 1356-1362, <https://doi.org/10.1126/science.aal4108>, 2017.

461 Archibald, S., Roy, D. P., van Wilgen, B. W., and Scholes, R. J.: What limits fire? An
462 examination of drivers of burnt area in Southern Africa, *Global Change Biology*, 15, 613-630,
463 [doi:10.1111/j.1365-2486.2008.01754.x](https://doi.org/10.1111/j.1365-2486.2008.01754.x), 2009.

464 Bachelet, D., Lenihan, J. M., Daly, C., and Neilson, R. P.: Interactions between fire, grazing and
465 climate change at Wind Cave National Park, SD, *Ecological Modelling*, 134, 229–244,
466 [https://doi.org/10.1016/S0304-3800\(00\)00343-4](https://doi.org/10.1016/S0304-3800(00)00343-4), 2000.

467 Bickel, P. J. and Doksum, K. A.: *Mathematical Statistics: Basic Ideas and Selected Topics*,
468 Volume I, Second Edition (Chapman & Hall/CRC Texts in Statistical Science) 2nd Edition.
469 (Mathematical Statistics | Taylor & Francis Group), 2015.

470 Bromley, L.: Relating violence to MODIS fire detections in Darfur Sudan, *International Journal*
471 *of Remote Sensing*, 31 (9), 2277–2292, <https://doi.org/10.1080/01431160902953909>, 2010.

472 Brooks, M. E., Kristensen, K., van Benthem, K. J., Magnusson, A., Berg, C. W., Nielsen, A.,
473 Skaug, H. J., Machler, M. and Bolker, B. M.: glmmTMB balances speed and flexibility
474 among packages for zero-inflated generalized linear mixed modeling, *The R Journal*, 9(2),
475 378-400, 2017.

476 Caracciolo, D., Istanbuloglu, E., and Noto, L.V.: An ecohydrological cellular automata model
477 investigation of juniper tree encroachment in a western north American landscape,
478 *Ecosystems*, 20, 1104-1123, <https://doi.org/10.1007/s10021-016-0096-6>, 2017.

479 Chang, J. F., Viovy, N., Vuichard, N., Ciais, P., Wang, T., Cozic, A., Lardy, R., Graux, A.-L, Klumpp,
480 K., Martin, R., and Soussana, J. F.: Incorporating grassland management in ORCHIDEE: model
481 description and evaluation at 11 eddy-covariance sites in Europe, *Geosci. Model Dev.*, 6, 2165-2181,
482 <https://doi.org/10.5194/gmd-6-2165-2013>, 2013.

483 Chuvieco, E., Mouillot, F., van der Werf, G. R., San Miguel, J., Tanase, M., Koutsias, N.,
484 García, M., Yebra, M., Padilla, M., Gitas, I., Heil, A., Hawbaker, T. J., and Giglio, L.:
485 Historical background and current developments for mapping burned area from satellite Earth
486 observation, *Remote Sens. Environ.*, 225, 45-64, <https://doi.org/10.1016/j.rse.2019.02.013>,
487 2019.

488 Cordova, C. E., Kirsten, K. L., Scott, L., Meadows, M., and Lucke, A.: Multi-proxy evidence of
489 late Holocene paleoenvironmental change at Princessvlei, South Africa, The effect of fire,
490 herbivores and humans, *Quaternary Science Reviews*, 221,
491 <https://doi.org/10.1016/j.quascirev.2019.105896>, 2019.

- 492 Cowtan, K. and Way, R. G.: Coverage bias in the HadCRUT4 temperature series and its impact
493 on recent temperature trends, *Q. J. R. Meteorol. Soc.*, 140, 1935-1944,
494 <https://doi.org/10.1002/qj.2297>, 2014.
- 495 Dangal, S. R. S., Tian, H., Lu, C., Ren, W., Pan, S., Yang, J., Di Cosmo, N., and Hessl, A.:
496 Integrating herbivore population dynamics into a global land biosphere model: plugging
497 animals into the earth system, *Journal of advances in modeling earth systems*, 9, 2920-2945,
498 <https://doi.org/10.1002/2016MS000904>, 2017.
- 499 Dubinin, M., Luschekina, A., and Radeloff, V. C.: Climate, livestock, and vegetation: what
500 drives fire increase in the arid ecosystems of southern Russia? *Ecosystems*, 14, 547-562,
501 [https://doi: 10.1007/s10021-011-9427-9](https://doi:10.1007/s10021-011-9427-9), 2011.
- 502 Evangeliou, N., Balkanski, Y., Hao, W. M., Petkov, A., Silverstein, R. P., Corley, R., Nordgren,
503 B. L., Urbanski, S. P., Eckhardt, S., Stohl, A., Tunved, P., Crepinsek, S., Jefferson, A.,
504 Sharma, S., Nøjgaard, J. K., and Skov, H.: Wildfires in northern Eurasia affect the budget of
505 black carbon in the Arctic – a 12-year retrospective synopsis (2002–2013), *Atmos. Chem.*
506 *Phys.*, 16, 7587-7604, <https://doi.org/10.5194/acp-16-7587-2016>, 2016.
- 507 Food and Agriculture Organization FAOSTAT Live Animals Database,
508 <http://www.fao.org/faostat/en/#home>, 2016.
- 509 Friedl, M. A., Sulla-Menashe, D., Tan, B., Schneider, A., Ramankutty, N., Sibley, A., and
510 Huang, X.: MODIS collection 5 global land cover: algorithm refinements and characterization
511 of new datasets, *Remote Sens. Environ.*, 114, 168-182,
512 <https://doi.org/10.1016/j.rse.2009.08.016>, 2010.
- 513 Fyfe, J. C., Gillett, N. P., and Zwiers, F. W.: Overestimated global warming over the past 20
514 years. *Nature Clim Change*, 3, 767-769, <https://doi.org/10.1038/nclimate1972>, 2013.
- 515 Fyfe, J. C., Meehl, G., England, M. et al.: Making sense of the early-2000s warming slowdown.
516 *Nature Clim Change* 6, 224–228, <https://doi.org/10.1038/nclimate2938>, 2016.
- 517 Gedalof, Z., Peterson, D. L., and Mantua, N. J.: Atmospheric, climatic, and ecological controls
518 on extreme wildfire years in the northwestern United States, *Ecological Applications*, 15,
519 154–174, <https://doi.org/10.1890/03-5116>, 2005.
- 520 Giglio, L., Randerson, J. T., and van der Werf, G. R.: Analysis of daily, monthly, and annual
521 burned area using the fourth-generation global fire emissions database (GFED4), *J. Geophys.*
522 *Res. Biogeosci.*, 118, 317–328, <https://doi:10.1002/jgrg.20042>, 2013.
- 523 Giglio, L., Boschetti, L., Roy, D., Humber, M. L., and Justice, C. O.: The collection 6 MODIS
524 burned are mapping algorithm and product, *Remote Sens. Environ.*, 217, 72-85,
525 <https://doi.org/10.1016/j.rse.2018.08.005>, 2018.
- 526 Goetz, S. J., MacK, M. C., Gurney, K. R., Randerson, J. T., and Houghton, R. A.: Ecosystem
527 responses to recent climate change and fire disturbance at northern high latitudes:
528 observations and model results contrasting northern Eurasia and North America, *Environ.*
529 *Res. Lett.*, 2, 045031, <https://doi.org/10.1088/1748-9326/2/4/045031>, 2007.
- 530 Goldammer, J. G., Stocks, B. J., Sukhinin, A. I., and Ponomarev, E.: Current fire regimes,
531 impacts and likely challenges - II: forest fires in Russia - past and current trends. in
532 *Vegetation Fires and Global Change*, Goldammer, J. G., Ed., 51-78, 2013.
- 533 Groisman, P. Ya., Sherstyukov, B. G., Razuvaev, V. N., Knight, R. W., Enloe, J. G.,
534 Stroumentova, N. S., Whitfield, P. H., Førland, E., Hannsen-Bauer, I., Tuomenvirta, H.,
535 Aleksandersson, H., Mescherskaya, A. V., and Karl, T. R.: Potential forest fire danger over
536 Northern Eurasia: Changes during the 20th century, *Global and Planetary Change*, 56, 371-
537 386, <https://doi.org/10.1016/j.gloplacha.2006.07.029>, 2007.

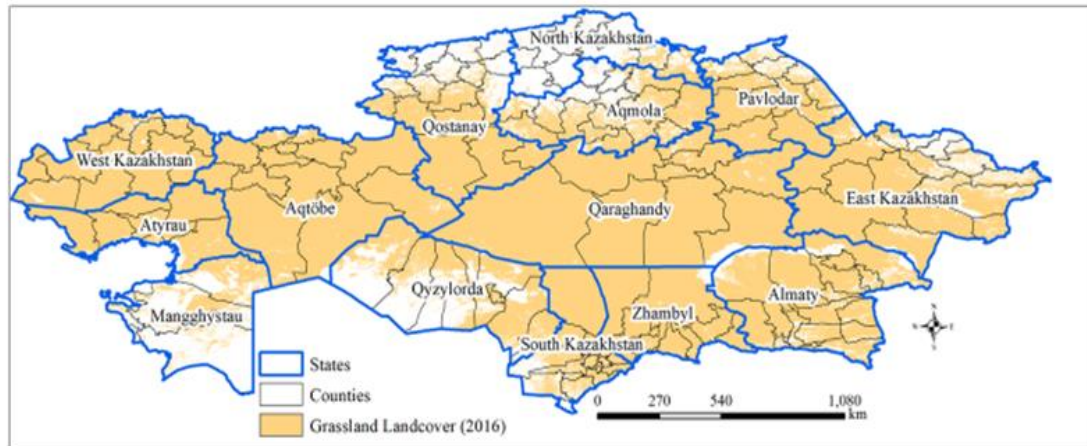
- 538 Hantson, S., Arneth, A., Harrison, S. P., Kelley, D. I., Prentice, I. C., Rabin, S. S., Archibald, S.,
539 Mouillot, F., Arnold, S. R., Artaxo, P., Bachelet, D., Ciais, P., Forrest, M., Friedlingstein, P.,
540 Hickler, T., Kaplan, J. O., Kloster, S., Knorr, W., Lasslop, G., Li, F., Mangeon, S., Melton, J.
541 R., Meyn, A., Sitch, S., Spessa, A., van der Werf, G. R., Voulgarakis, A., and Yue, C.: The
542 status and challenge of global fire modelling, *Biogeosciences*, 13, 3359-3375, DOI:
543 10.5194/bg-13-3359-2016, 2016.
- 544 Hao, W. M. and Liu, M.-H.: Spatial and temporal distribution of tropical biomass burning,
545 *Global Biogeochem. Cy.*, 8, 495-503, <https://doi.org/10.1029/94GB02086>, 1994.
- 546 Hao, W.M., Petkov, A., Nordgren, B., Corley, R.E., and Urbanski, S.P.: Comparison of MODIS-
547 derived burned area algorithm with Landsat images in eastern Siberia, Russia. in: *Proceedings*
548 *of the 2012 International Emission Inventory Conference: Emission Inventories – Meeting the*
549 *Challenges Posed by Emerging Global, National, Regional and Local Air Quality Issues*,
550 Tampa, FL, 13–16 August, 2012.
- 551 Hao, W. M., Petkov, A., Nordgren, B. L., Corley, R. E., Silverstein, R. P., Urbanski, S. P.,
552 Evangeliou, N., Balkanski, Y., and Kinder, B. L.: Daily black carbon emissions from fires in
553 northern Eurasia for 2002–2015, *Geosci. Model Dev.*, 9, 4461-4474, [www.geosci-model-](http://www.geosci-model-dev.net/9/4461/2016/doi:10.5194/gmd-9-4461-2016)
554 [dev.net/9/4461/2016/doi:10.5194/gmd-9-4461-2016](http://www.geosci-model-dev.net/9/4461/2016/doi:10.5194/gmd-9-4461-2016), 2016a.
- 555 Hao, W. M., Petkov, A., Nordgren, B. L., Corley, R. E., Silverstein, R. P., and Urbanski, S. P.:
556 Daily black carbon emissions data from fires in Northern Eurasia for 2002–2015, *Forest*
557 *Service Research Data Archive*, <https://doi.org/10.2737/RDS-2016-0036>, 2016b.
- 558 Holdo, R. M., Holt, R. D., and Fryxell, J. M.: Grazers, browsers, and fire influence the extent and
559 spatial pattern of tree cover in the Serengeti, *Ecological Applications*, 19, 95-109,
560 <https://doi.org/10.1890/07-1954.1>, 2009.
- 561 Huber, P. J.: *Robust Statistics*, in *Wiley series in probability and mathematics statistics*, John
562 Wiley & Sons, 1981
- 563 IPCC, 2013: *Climate Change 2013: The Physical Science Basis. Contribution of Working Group*
564 *I to the Fifth Assessment Report of the Intergovernmental Panel on Climate Change* [Stocker,
565 T.F., D. Qin, G.-K. Plattner, M. Tignor, S.K. Allen, J. Boschung, A. Nauels, Y. Xia, V. Bex
566 and P.M. Midgley (eds.)]. Cambridge University Press, Cambridge, United Kingdom and
567 New York, NY, USA, 1535 pp., 2013.
- 568 IPCC, 2014: *Climate Change 2014: Synthesis Report. Contribution of Working Groups I, II and*
569 *III to the Fifth Assessment Report of the Intergovernmental Panel on Climate Change* [Core
570 Writing Team, R.K. Pachauri and L.A. Meyer (eds.)]. IPCC, Geneva, Switzerland, 151 pp.,
571 2014.
- 572 Jolly, W. M., Cochrane, M. A., Freeborn, P. H., Holden, Z. A., Brown, T. J., Williamson, G. J.,
573 and Bowman, D. M. J. S.: Climate-induced variations in global wildfire danger from 1979 to
574 2013, *Nature communications*, 6, 7537, <https://doi.org/10.1038/ncomms8537>, 2015.
- 575 Jones, P. D., Parker, D. E., Osborn, T. J., and Briffa, K. R.: Global and hemispheric temperature
576 anomalies: land and marine instrumental records (1850 - 2015). United States: N. p.,
577 2016. Web. doi:10.3334/CDIAC/cli.002, 2016.
- 578 Kendall, M. G: A new measure of rank correlation, *Biometrika*, 30 (1–2), 81–93, 1938.
- 579 Kharuk, V. I., Ranson, K. Jon, and Dvinskaya, M. L.: Wildfires dynamic in larch dominance
580 zone, *Geophys. Res. Lett.*, 35, L01402, <https://doi.org/10.1029/2007GL032291>, 2008.
- 581 Kloster, S., Mahowald, N. M., Randerson, J. T., Thornton, P. E., Hoffman, F. M., Levis, S.,
582 Lawrence, P. J., Feddema, J. J., Oleson, K. W., and Lawrence, D. M.: Fire dynamics during

- 583 the 20th century simulated by the community land model, *Biogeosciences*, 7, 1877-1902,
584 <https://doi.org/10.5194/bg-7-1877-2010>, 2010.
- 585 Koerner, S. E. and Collins, S. L.: Interactive effects of grazing, drought, and fire on grassland
586 plant communities in North America and South Africa, *Ecology*, 95, 98–109,
587 <https://doi.org/10.1890/13-0526.1>, 2014.
- 588 Krawchuck, M. A. and Moritz, M. A.: Constraints on global fire activity vary across a resource
589 gradient, *Ecology*, 92, 121-132, <https://doi.org/10.1890/09-1843.1>, 2011.
- 590 Lebed, L. V., Qi, J., and Heilman, P.: An ecological assessment of pasturelands in the Balkhash
591 area of Kazakhstan with remote sensing and models, *Env. Res. Lett.*, 7,
592 DOI: 10.1088/1748-9326/7/2/025203, 2012.
- 593 Liu, Yi. Y., Evans, J. P., McCabe, M. F., de Jeu, R. A. M., van Dijk, A. I. J. M., Dolman, A. J.,
594 and Saizen, I.: Changing climate and overgrazing are decimating Mongolian steppes, *PLoS*
595 *ONE* 8, e57599, <https://doi.org/10.1371/journal.pone.0057599>, 2013.
- 596 MANE: National Economy of the Republic of Kazakhstan Committee on Statistics. 2019.
597 http://www.stat.gov.kz/faces/wcnav_externalId/homeNumbersAgriculture. Last Visited April
598 28, 2019.
- 599 Marlon, J. R., Bartlein, P. J., Carcaillet, C., Gavin, D. G., Harrison, S. P., Higuera, P. E., Joos, F.,
600 Power, M. J., and Prentice, I. C.: Climate and human influences on global biomass burning
601 over the past two millennia, *Nature Geosci*, 1, 697–702, <https://doi.org/10.1038/ngeo313>,
602 2008.
- 603 Moritz, M. A., Morais, M. E., Summerell, L. A., Carlson, J. M., and Doyle, J.: Wildfires,
604 complexity, and highly optimized tolerance, *Proc. Natl. Acad. Sci. USA*, 102, 17912-17917,
605 <https://doi.org/10.1073/pnas.0508985102>, 2005.
- 606 Motesharrei, S., Rivas, J., Kalnay, E., Asrar, G. R., Busalacchi, A. J., Cahalan, R. F., Cane, M.
607 A., Colwell, R. R., Feng, K., Franklin, R. S., Hubacek, K., Miralles-Wilhelm, F., Miyoshi, T.,
608 Ruth, M., Sagdeev, R., Shirmohammadi, A., Shukla, J., Srebric, J., Yakovenko, V. M., and
609 Zeng, N.: Modeling sustainability: population, inequality, consumption, and bidirectional
610 coupling of the earth and human systems, *National Science Review*, 3(4): 470-494.
611 <https://doi.org/10.1093/nsr/nww081>, 2016.
- 612 Mouillot, F. and Field, C. B.: Fire history and the global carbon budget: a 1° x 1° fire history
613 reconstruction for the 20th century, *Global Change Biology*, 11, 398-420,
614 <https://doi.org/10.1111/j.1365-2486.2005.00920.x>, 2005.
- 615 Mouillot, F., Schultz, M. G., Yue, C., Cadule, P., Tansey, K., Ciais, P., and Chuvieco, E.: Ten
616 years of global burned area products from spaceborne remote sensing - a review: analysis of
617 user needs and recommendations for future developments, *International Journal of Applied*
618 *Earth Observation and Geoinformation*, , 26, 64-79, <https://doi.org/10.1016/j.jag.2013.05.014>,
619 2014.
- 620 Nandintsetseg, B., Shinoda, M., Du, C., and Munkhjargal, E: Cold-season disasters on the
621 Eurasian steppes: Climate-driven or man-made, *Sci Rep*, 8, 14769,
622 <https://doi.org/10.1038/s41598-018-33046-1>, 2018.
- 623 NASA Global Climate Change, <https://climate.nasa.gov/vital-signs/global-temperature/>, last
624 access, September 12, 2019.
- 625 Neumann, M., Braun, A., Heinke, E.-M., Saqalli, M., and Srblijinovic, A.: Challenges in
626 modelling social conflicts: Grappling with polysemy, *Journal of Artificial Societies and Social*
627 *Simulation*, 14 (3), 9, DOI: 10.18564/jasss.1818, 2011.
- 628

- 629 Otón, G., Ramo, R., Lizundia-Loiola, J., and Chuvieco, E.: Global detection of long-term (1982–
630 2017) burned area with AVHRR-LTDR data, *Remote Sens.*, 11, 2079,
631 <https://doi.org/10.3390/rs11182079>, 2019.
- 632 Pachzelt, A., Forrest, M., Rammig, A., Higgins, S. I., and Hickler, T.: Potential impact of large
633 ungulate grazers on African vegetation, carbon storage and fire regimes, *Global ecology and*
634 *biogeography*, 24, 991-1002, <https://doi.org/10.1111/geb.12313>, 2015.
- 635 Palmer, W., Meteorological drought, U.S. Department of Commerce, Weather Bureau, Research
636 Paper, 45, 1965.
- 637 Pausas, J. G. and Keeley, J. E.: Abrupt climate-independent fire regime changes, *Ecosystems*
638 17,1109-1120, <https://doi.org/10.1007/s10021-014-9773-5>, 2014.
- 639 Pausas, J. G. and Ribeiro, E.: The global fire-productivity relationship, *Global ecology and*
640 *biogeography*, 22, 728-736, <https://doi.org/10.1111/geb.12043>, 2013.
- 641 Perry, B. D., Grace, D., and Sones, K.: Current drivers and future directions of global livestock
642 disease dynamics, *Proc. Natl. Acad. Sci. USA.* 110 (52), 20871-20877,
643 <https://doi.org/10.1073/pnas.1012953108>, 2013.
- 644 Pongratz, J., Dolman, H., Don, A., Erb, K.-H., Fuchs, R., Herold, M., Jones, C., Kuemmerle, T.,
645 Luysaert, S., Meyfroidt, P., and Naudts, K.: Models meet data: Challenges and opportunities
646 in implementing land management in earth system models. *Global change biology*, 24, 1470-
647 1487, <https://doi.org/10.1111/gcb.13988>, 2018.
- 648 Prestele, R., Arneth, A., Bondeau, A., De Noblet-Ducoudre, N., Pugh, T. A. M., Sitch, S.,
649 Stehfest, E., and Verburg, P. H.: Current challenges of implementing anthropogenic land-use
650 and land-cover change in models contributing to climate change assessments, *Earth system*
651 *dynamics*, 8, 369-386, doi:10.5194/esd-8-369-2017, 2017.
- 652 R Core Team: R: A language and environment for statistical computing. R Foundation for
653 Statistical Computing, Vienna, Austria. URL <https://www.R-project.org/>, 2019.
- 654 Reeves, M. C.: Development of the rangeland vegetation simulator: A module of the forest
655 vegetation simulator. Final report to the Joint Fire Science Program, Boise, Idaho, 2016.
- 656 Reeves, M. C., Hanberry, H., Wilmer, N., Kaplan, W. K., and Lauenroth, An assessment of
657 production trends on the Great Plains from 1984 to 2017, *Rangeland Ecology and*
658 *Management*. in press.
- 659 Riley, K. L., Abatzoglou, J. T., Grenfell, I. C., Klene, A. E., and Heinsch, F. A.: The relationship
660 of large fire occurrence with drought and fire danger indices in the western USA, 1984–2008,
661 *International Journal of Wildland Fire*, 22, 894–909, <https://doi.org/10.1071/WF12149>,
662 2013.
- 663 Robinson, S. and Milner-Gulland, E. J.: Political change and factors limiting numbers of wild
664 and domestic ungulates in Kazakhstan, *Human Ecology*, 31, 87-110,
665 <https://doi.org/10.1023/A:1022834224257>, 2003.
- 666 Rolinski, S., Müller, C., Heinke, J., Weindl, I., Biewald, A., Bodirsky, B. L., Bondeau, A.,
667 Boons-Prins, E. R., Bouwman, A. F., Leffelaar, P. A., te Roller, J. A., Schaphoff, S., and
668 Thonicke, K.: Modeling vegetation and carbon dynamics of managed grasslands at the global
669 scale with LPJmL 3.6 . *Geosci. Model Dev.*, 11, 429-451, <https://doi.org/10.5194/gmd-11-429-2018>, 2018.
- 671 Roy, D. P., Boschetti, L., Justice, C.O., and Ju, J.: The collection 5 MODIS burned area product
672 – Global evaluation by comparison with the MODIS active fire product, *Remote Sens.*
673 *Environ.*, 112, 3690-3707, <https://doi.org/10.1016/j.rse.2008.05.013>, 2008.

- 674 Santin-Janin, H., Garel, M., Chapuis, J.-L., and Pontier, D.: Assessing the performance of NDVI
675 as a proxy for plant biomass using non-linear models: a case study on the Kerguelen
676 archipelago, *Polar Biol*, 32, 861–871, <https://doi.org/10.1007/s00300-009-0586-5>, 2009.
- 677 Sato, T. and Nakamura, T.: Intensification of hot Eurasian summers by climate change and land–
678 atmosphere interactions, *Sci Rep*, 9, 10866, <https://doi.org/10.1038/s41598-019-47291-5>,
679 2019.
- 680 Seneviratne, S. I., Donat, M. G., Mueller, B., and Alexander, L.V.: No pause in the increase of
681 hot temperature extremes, *Nature Climate Change*, 4, 161-163,
682 <https://doi.org/10.1038/nclimate2206>, 2014.
- 683 Tachiiri, K and Shinoda, M.: Quantitative risk assessment for future meteorological disasters
684 reduced livestock mortality in Mongolia, *Climatic Change*, 113, 867-882,
685 <https://doi.org/10.1007/s10584-011-0365-5>, 2012.
- 686 Trenberth, K. E., Fasullo, J. T., Branstator, G., and Phillips, A. S.: Seasonal aspects of the recent
687 pause in surface warming, *Nature Climate Change*, 4, 911-916,
688 <https://doi.org/10.1038/nclimate2341>, 2014.
- 689 Trendberth, K. E., Fasullo, J. T., and Shepherd, T. G.: Attribution of climate extreme events,
690 *Nature Climate Change*, 5, 725-730, <https://doi.org/10.1038/nclimate2657>, 2015.
- 691 Vandergert, P. and Newell, J. P.: Illegal logging in the Russian Far East and Siberia, *Int. For.*
692 *Rev.*, 5, 303-306, <https://doi.org/10.1505/IFOR.5.3.303.19150>, 2003.
- 693 Venables W. N. and Ripley, B. D.: *Modern Applied Statistics with S*, Fourth edition. Springer,
694 New York. ISBN 0-387-95457-0, 2002.
- 695 Vigan, A., Lasseur, J., Benoit, M., Mouillot, F., Eugène, M., Mansard, L., Vigne, M., Lecomte,
696 P., and Dutilly, C.: Evaluating livestock mobility as a strategy for climate change mitigation:
697 combining models to address the specificities of pastoral systems, *Agriculture, Ecosystems &*
698 *Environment*, 242, 89-101, <https://doi.org/10.1016/j.agee.2017.03.020>, 2017.
- 699 Vrieling, A., Meroni, M., Mude, A. G., Chantararat, S., Ummenhofer, C. C., and de Bie, K.: Early
700 assessment of seasonal forage availability for mitigating the impact of drought on East
701 African pastoralists, *Remote Sens. Environ.*, 174, 44-55,
702 <https://doi.org/10.1016/j.rse.2015.12.003>, 2016.
- 703 Xu, Y., Zhang, Y., Chen, J., and John, R., J.: Livestock dynamics under changing economy and
704 climate in Mongolia, *Land Use Policy*, 88, 104120,
705 <https://doi.org/10.1016/j.landusepol.2019.104120>, 2019.
- 706 Yue, C., Ciais, P., Cadule, P., Thonicke, K., Archibald, S., Poulter, B., Hao, W. M., Hantson, S.,
707 Mouillot, F., Friedlingstein, P., Maignan, F., and Viovy, N.: Modelling the role of fires in the
708 terrestrial carbon balance by incorporating SPITFIRE into the global vegetation model
709 ORCHIDEE- Part 1: Simulating historical global burned area and fire regimes. *Geosci.*
710 *Model Dev.*, 7, 2747-2767, <https://doi.org/10.5194/gmd-7-2747-2014>, 2014.

[Type here]



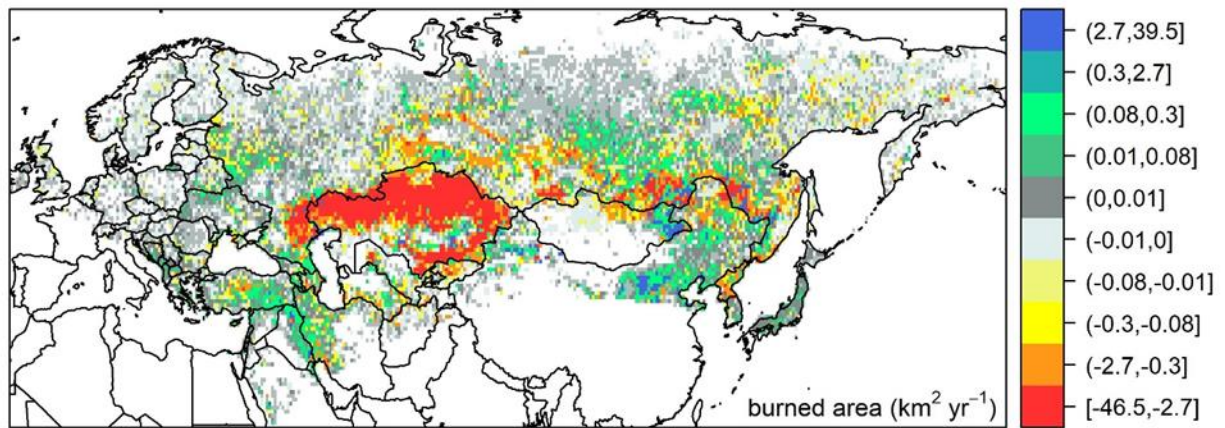
712

713 **Figure 1.** The distribution of grassland cover in Kazakhstan with counties and states shown as
714 administrative boundaries.

715

716

[Type here]

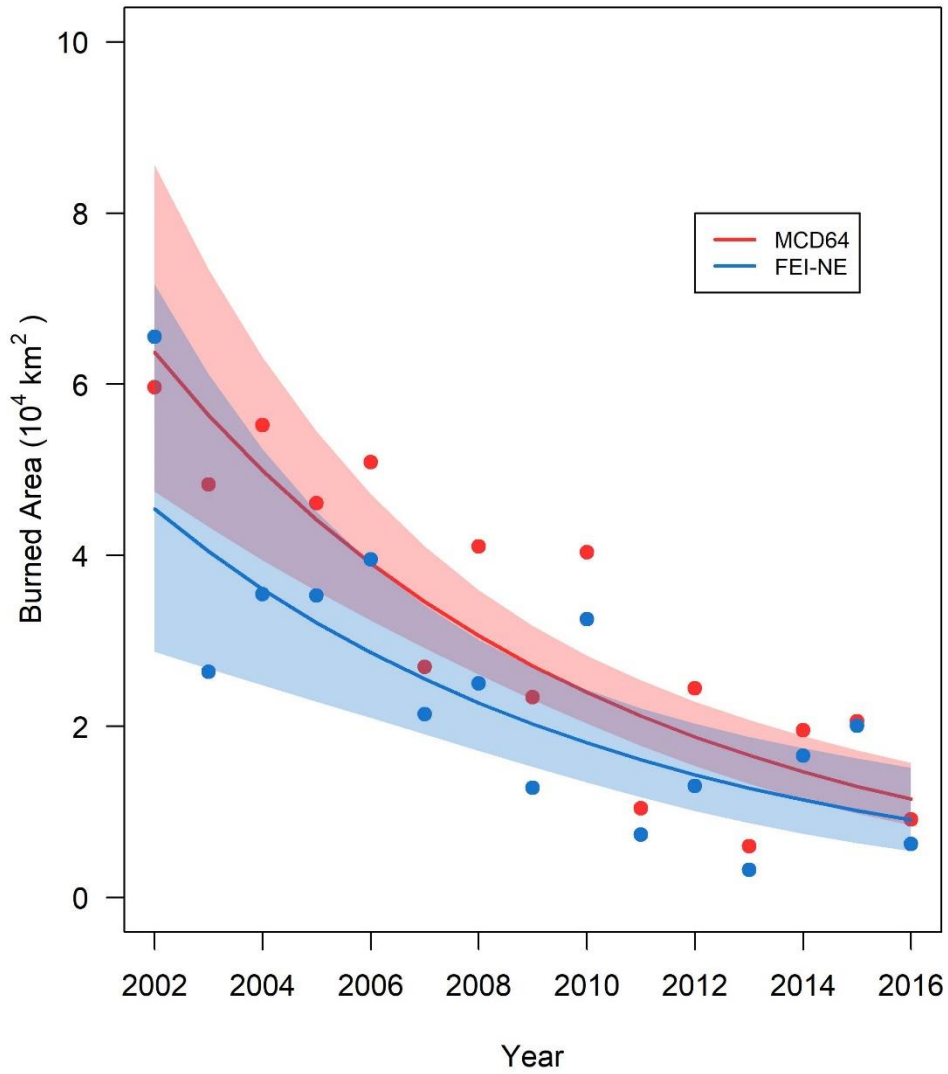


717
718
719
720
721
722
723
724
725
726
727
728
729
730
731
732
733

Figure 2. Spatial distributions of robust linear trends of the area burned for each $0.5^\circ \times 0.5^\circ$ grid cell in northern Eurasia from 2002 to 2016. The border of Kazakhstan is also illustrated in Figure 1.

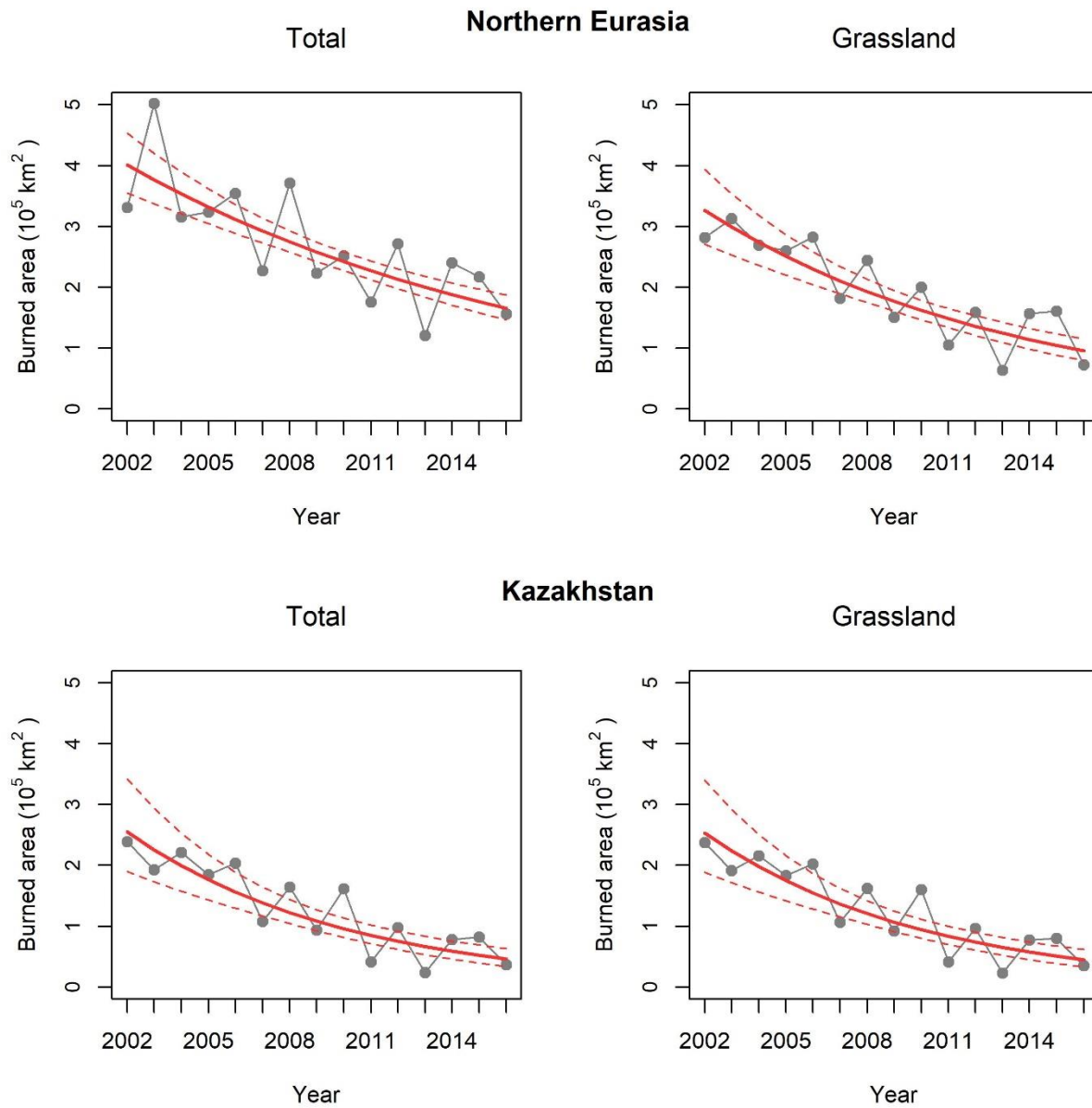
734

735



736

737 **Figure 3.** Comparison of burned areas between the dataset of Forest Service Fire Emission
738 Inventory – northern Eurasia (FEI-NE) and MODIS MCD64. The FEI-NE (blue) and MCD64
739 (pink) bands illustrate the 95% confidence intervals.



741

742

743 **Figure 4.** Declining trends of the total area and grassland area burned in Northern Eurasia

744 (including Kazakhstan) and Kazakhstan from 2002 to 2016. The solid lines are the trend lines

745 and the dotted lines are 95% confidence intervals.

746

747

748

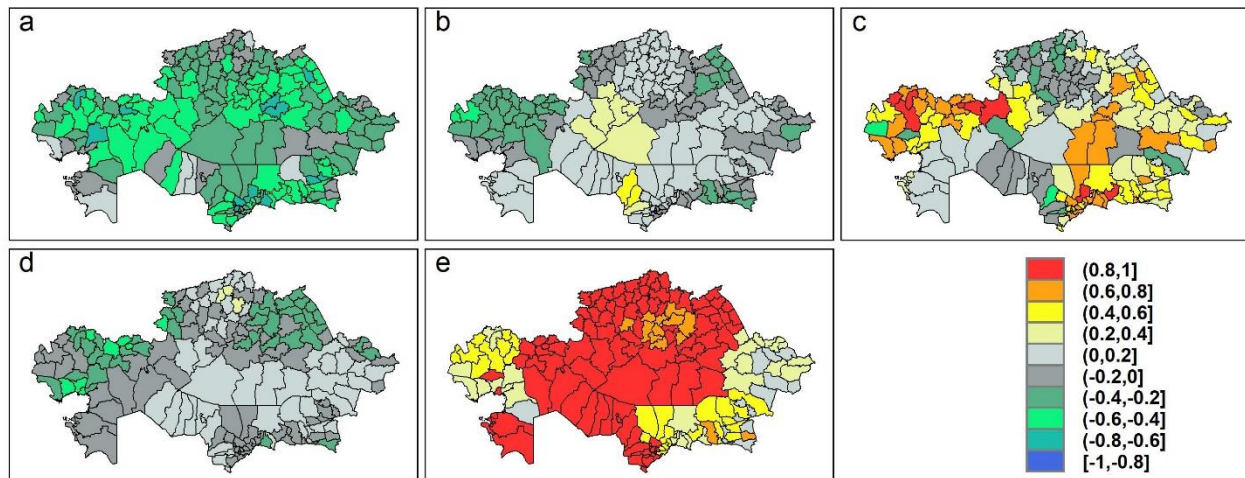
749

750

751

752

[Type here]



753

754

755

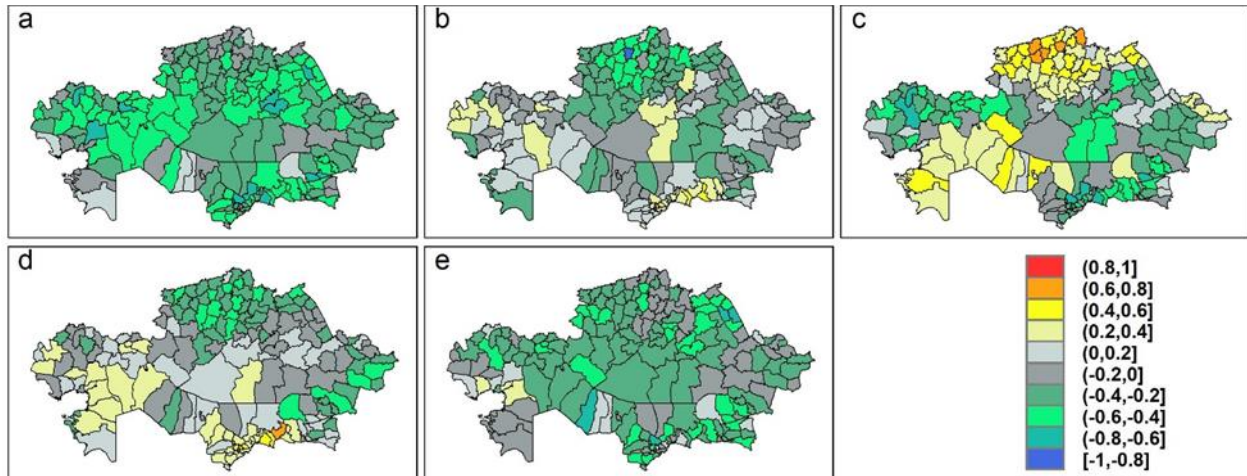
756

757

758

Figure 5. Pairwise robust rank correlations of year with (a) fraction of burned area, (b) PDSI, (c) proportion of grassland layer, (d) ANPP and (e) livestock density without considering their interactions.

[Type here]

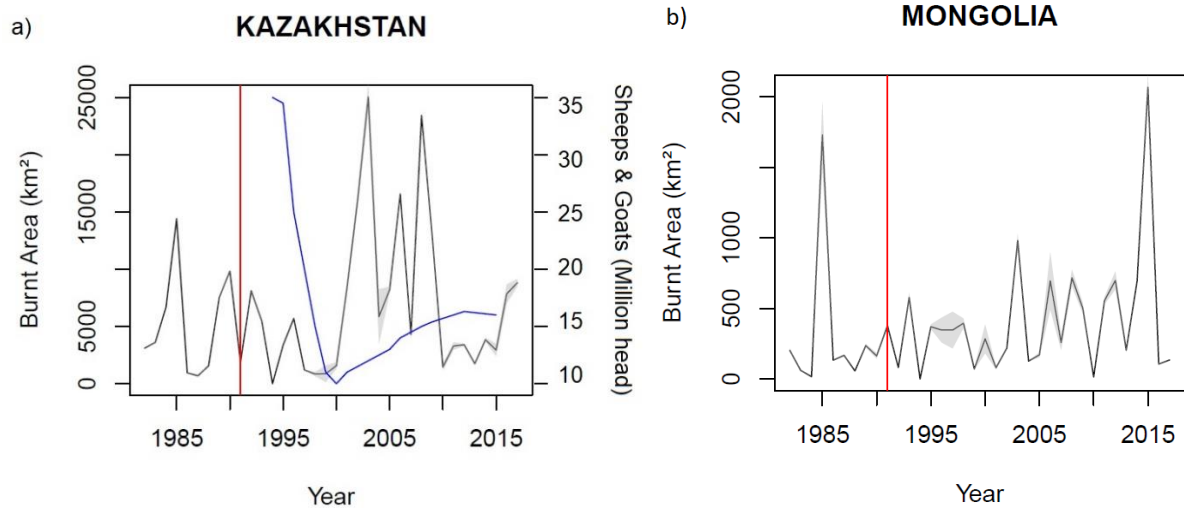


759
760

761 **Figure 6.** Pairwise robust rank correlations of fraction of burned area with (a) year, (b) PDSI, (c)
762 proportion of grassland layer, (d) ANPP and (e) livestock density without considering their
763 interactions.

764
765
766
767
768
769
770
771
772
773
774
775
776
777
778
779
780
781
782
783
784
785
786
787
788

[Type here]



789
790
791
792
793
794
795
796

Figure 7. Yearly burned area (in km²) in (a) Kazakstan and (b) Mongolia for the 1982-2017 period based on the AVHRR remotely sensed burned area Long Term Data Record_Climate Change Initiative (FIRECCILT10) (<https://www.mdpi.com/2072-4292/11/18/2079>, Otón et al., 2019). The black line represents mean burned fraction and grey area the burned area 95% uncertainty delivered by FIRECCILT10. The blue line represents the sheep and goat population for the 1994-2014 period. The red line represents the end year of the Soviet Union. Note: the scale of the area burned (y-axis) in Kazakstan (a) is 10 times greater than that in Mongolia (b).

Table 1. The area burned in forest, grassland, shrubland and savanna in geographic regions from 2002 to 2016. The data of the area burned in Kazakhstan are listed for comparison only, and are not included in the tabulation.

Region	Burned Area (km ²)															Total
	2002	2003	2004	2005	2006	2007	2008	2009	2010	2011	2012	2013	2014	2015	2016	
Forest (Evergreen Needleleaf, Evergreen Broadleaf, Deciduous Needleleaf, Deciduous Broadleaf, Mixed)																
Russia	26,458	99,944	16,715	20,561	32,929	23,731	72,671	33,356	19,309	43,910	73,920	29,791	62,701	38,511	51,718	646,223
East Asia	1,483	9,697	6,368	4,202	2,814	2,524	4,597	6,676	1,258	3,379	4,189	1,819	3,151	2,944	1,336	56,436
Central & Western Asia	131	206	367	259	388	469	641	389	348	159	321	307	517	726	455	5,684
Europe	376	1,172	467	592	491	1,170	850	863	328	1,206	2,307	537	1,224	1,756	575	13,911
Subtotal	28,448	111,019	23,917	25,613	36,623	27,894	78,758	41,283	21,243	48,653	80,736	32,455	67,592	43,937	54,084	722,254
Grassland																
Russia	32,019	97,754	33,372	61,755	62,973	55,220	65,144	46,375	30,634	43,760	37,261	21,114	51,745	49,857	22,178	711,160
East Asia	10,643	21,235	15,551	12,433	14,456	16,819	15,278	11,259	8,097	18,716	23,870	18,123	26,689	29,361	13,962	256,492
Central & Western Asia	239,160	193,580	220,080	185,531	204,627	109,248	163,814	92,592	161,668	41,943	97,363	24,364	78,203	81,517	36,369	1,930,057
Europe	128	271	108	555	241	616	325	217	104	401	526	150	186	237	179	4,242
Subtotal	281,948	312,840	269,112	260,273	282,296	181,903	244,560	150,443	200,503	104,819	159,021	63,752	156,822	160,972	72,688	2,901,951
Kazakhstan	237,335	191,466	215,977	182,968	202,292	106,558	162,474	91,873	160,318	40,995	96,420	23,195	76,977	80,251	35,249	1,904,348
Shrubland (Closed Shrubland and Open Shrubland)																
Russia	7,042	27,749	4,894	13,149	5,924	2,868	10,901	13,096	18,854	6,697	12,650	10,918	5,717	3,486	14,529	158,470
East Asia	337	79	264	828	934	675	790	645	375	914	796	193	317	153	191	7,490
Central & Western Asia	1,022	2,836	5,632	2,384	1,255	1,728	999	1,217	3,279	964	769	845	1,066	1,287	1,720	27,001
Europe	20	38	23	70	39	121	112	87	21	83	70	11	13	10	17	732
Subtotal	8,421	30,701	10,813	16,430	8,152	5,391	12,802	15,044	22,529	8,657	14,285	11,966	7,112	4,934	16,457	193,693
Savanna (Woody Savanna and Savanna)																
Russia	11,136	43,574	8,307	19,343	25,129	10,465	33,347	14,191	6,745	12,473	16,387	12,076	8,324	6,261	12,039	239,796
East Asia	589	3,504	3,257	1,275	1,564	694	1,268	1,349	465	611	660	205	147	510	131	16,226
Central & Western Asia	575	500	437	395	442	317	413	391	261	115	193	112	161	301	178	4,791
Europe	83	207	110	293	200	653	340	400	113	319	426	212	201	142	243	3,941
Subtotal	12,383	47,785	12,110	21,306	27,335	12,128	35,368	16,330	7,584	13,517	17,666	12,604	8,832	7,215	12,592	264,753
Total	331,199	502,346	315,951	323,621	354,405	227,317	371,488	223,100	251,859	175,646	271,707	120,777	240,358	217,058	155,820	4,082,650

Table 2. Model parameters and associated *p*-values.

<i>Parameter</i>	<i>Estimate</i>	<i>Std. Error</i>	<i>z</i>	<i>Pr(> z)</i>
Year * ANPP	-0.02	0.01	-4.03	<0.001
Year * PDSI	0.00	0.00	0.20	0.838
Year * Proportion Grass Area	-0.26	0.04	-6.77	<0.001
Year * Livestock Density (head km ⁻²)	1.04	0.61	1.70	0.089
ANPP * PDSI	-0.01	0.01	-0.92	0.360
ANPP * Proportion Grass Area	0.72	0.19	3.83	<0.001
ANPP * Livestock Density (head km ⁻²)	0.88	3.22	0.27	0.784
PDSI * Proportion Grass Area	-0.24	0.11	-2.20	0.028
PDSI * Livestock Density (head km ⁻²)	-3.30	1.62	-2.04	0.042
Proportion Grass Area * Livestock Density (head km ⁻²)	37.78	28.32	1.33	0.182

Estimate = parameter estimate from GLMM, Std. Error = standard error of parameter estimate,
 z = z -statistic, $\text{Pr}(>|z|)$ = p -value